JOURNAL OF MATERIALS RESEARCH AND TECHNOLOGY 2020;9(6):15788–15801

Available online at www.sciencedirect.com

jmr&t Journal of Materials Research and Technology

journal homepage: www.elsevier.com/locate/jmrt

Original Article

Statistical characterization and simulation of graphene-loaded polypyrrole composite electrical conductivity

Oladipo Folorunso [a,d,*], Yskandar Hamam [a,b], Rotimi Sadiku [c], Suprakas Sinha Ray [d,e], Gbolahan Joseph Adekoya [c]

[a] French South African Institute of Technology (F'SATI), Department of Electrical Engineering, Tshwane University of Technology, Pretoria 0001, South Africa

[b] École Supérieure d'Ingénieurs en Électrotechnique et Électronique, Cité Descartes, 2 Boulevard Blaise Pascal, Noisy-le-Grand, Paris 93160, France

[c] Institute of NanoEngineering Research (INER), Department of Chemical, Metallurgy and Material Engineering, Tshwane University of Technology, Pretoria 0001, South Africa

[d] Centre for Nanostructures and Advanced Materials, DSI-CSIR Nanotechnology Innovation Centre, Council for Scientific and Industrial Research, Pretoria 0001, South Africa

[e] Department of Chemical Sciences, University of Johannesburg, Doornfontein, Johannesburg 2028, South Africa

ARTICLE INFO

Article history:
Received 25 August 2020
Accepted 17 November 2020
Available online 24 November 2020

Keywords:
Polypyrrole
Graphene
Potential barrier
Interfacial effect and conductivity

ABSTRACT

In this study, an effective method has been described and adopted to quantify the diameter and length of graphene nanofiller. The experimentally measured graphene parameters were modelled by using the Weibull distribution. The fitted graphene nanofiller length and diameter were used to predict the electrical conductivity of the graphene-loaded polypyrrole. The reliability of the dispersion of the filler in the matrix is, aided by the adequate distribution of the filler. An analytical model was developed to study the conductivity of the polypyrrole-graphene (PPy-Gr) composite. In the model, the interfacial effect of the composite constituents was considered and the electrical conductivity of the composite was determined by the simple-sum method. The percolation threshold and the electrical conductivity dependencies of the composites were evaluated by concurrently varying the potential barrier, filler electrical conductivity and the interfacial thickness and the matrix conductivity. The current model produced results, which are in good agreement with experimental measurements of different polymer-composites. It is envisaged that the method employed in this study, can be extended to other polymer-filler mixture as a predictive, optimization and design tool, for polymer composites of any type.

* *Corresponding author.*
E-mail address: oladfol2013@gmail.com (O. Folorunso).

https://doi.org/10.1016/j.jmrt.2020.11.045

1. Introduction

Polypyrrole (PPy) is a conductive polymer, of which, its usability spans a range of applications, such as gas sensors, supercapacitors, rechargeable batteries, electromagnetic shielding, actuators, protective material against corrosion and biosensors [1–3]. For energy storage application, polypyrrole has excellent storage capability due to its strong binding energy with two-dimensional materials [4,5]. On the nanoscale level, PPy is highly porous; hence, it has the capacities to charge at a high rate, produce high power density, and it possesses a long life cycle. As an alternative to metals, PPy is lightweight, and its process of manufacturing is not complicated [6]. The emerging technology requires materials that are mechanically strong, a lightweight, good conductor of heat and electricity, chemically stable and less corrosive. The interests in PPy are due to its inherent good mechanical, electrical and chemical properties. The phase change (i.e. from insulator to conductor and conductor to insulator), which occurs when other materials are added to polymers, make them the indescribable materials for the future and the present engineering material [6].

Graphene is a crystalline carbonaceous nanomaterial. It has an experimental electron mobility of 15,000 $cm^2(Vs)^{-1}$ [7]. Graphene is single layer graphite, whose resistivity is lower than silver and possesses excellent thermal, optical, electrical and mechanical properties. For practical applications, the thickness of graphene must be adjusted by a suitable synthetic method in order to produce large-scale films. A generalized ion implantation method, for a largescale, high-quality synthesis of graphene films with controllable thickness, was experimented by Garaj et al. [8]. Electrochemical exfoliation, mechanical exfoliation, hydrothermal and directed-synthesis methods, have been applied to produce graphene [9–12]. The energy storage advantages of graphene have been attributed to its excellent electrical conductivity and mechanical integrity, high electron mobility, wide electrochemical window and large surface area [13,14].

By combining the superior properties of PPy and graphene, an enviable electrochemical anode material, is envisaged. This study aims at investigating the electrical conductivity of graphene-loaded PPy, by considering the interfacial effects of the fillers on the polymer. In addition, PPy conductivity, graphene conductivity and the potential barriers are parameters of interest, and they are studied as factors, which affect the conductivity of polymer-composites. The electrical conductivity of polymer-composites, using different fillers and different processing methods, have been widely investigated [15–20]. Generally, the network of filler and matrix, in contact, forms the electrical conductivity of polymer-composite. This network usually follows a percolation law with respect to volume fraction. Among others, the electrical conductivity of polymer-composites depends on the filler loadings: as the filler changes from zero to a certain % (percentage) level of inclusion, the state of the polymer changes from an insulator to semiconductor or even conductor. From the literature, the parameters elucidated to have effects on the electrical conductivity of polymer-composites, have been explained to include: shapes, carrier tunneling, fiber types and the extent of inclusion and polymer conductivity, packing factors, orientation angle, etc. [15,21–24].

The percolation theory has been statistically, thermodynamically, structurally and geometrically, modelled to predict the conductivity of a variety of fillers, dispersed in different polymers. Mathematical and empirical rules have also been utilized to investigate how the properties of polymers can be varied by fillers inclusion. Mammunya, Clingerman, McCullough, Kirkpatrick and Sigmoidal, are examples of statistical, thermodynamics, geometric and structured electrical conductivity models for polymer-composites [25]. Maxwell, Bruggman, Pal, are some of the examples of the mathematical models, while the logarithm rule is an empirical rule model [26]. The success of these models can be credited to some certain filler types; however, they cannot be generalized to measure the conductivity of polymer-composites. Another important omission in the afore-mentioned models is the interfacial particle effect. It is believed that since the interaction between polymer and fillers, occurs at the nano-level, then, their electrical conductivity predictions must include the effects of the interface between filler-to-filler and the matrix-to-filler [6].

Moreover, the random dispersion of filler in the polymer matrix without adequate and proper characterization of their sizes may introduce errors in the simulation results [27]. An investigation conducted by Wang et al. [28], showed that nanocomposites would perform poorly if fillers are heterogeneously dispersed in the polymer matrix. Hence, the statistical distribution of the filler size is vital to obtaining reliable electrical conductivity models for polymer-composites.

Yan et al. [29], reported that classical predictive models lack sufficient parameters to explain the agreement of experimental data with theoretical values. In Yan et al. [29] opinion, an electrical conductivity model is expected to consider the van der Waals interactions of the matrix and the fillers. This is because an interface that is formed during the interaction would have an effect on the overall conductivity of the composite. The role of tunneling resistance in the electrical conductivity of polymer-composite by using an analytical model, was investigated by Yu et al., [20]. Tunneling conductance between the shells of fillers was found to play an important role in the electron transport in polymer-composite conductivity, especially when fillers are at low concentrations. Venugopal et al. [19], reported the effects of contact resistance in multilayer graphene devices by employing an analytical model. Their results showed that contact resistance contributes to the total resistance of graphene-polymer composite; therefore, a useful conductivity model should incorporate the impact of this resistance for the effective electrical conductivity of polymer-composites. A multi-scale approach was used by Senghor et al. [30], to predict the overall electrical resistivity of polymer-composites. In this approach, filler orientation and the anisotropic properties of the materials were considered. A finite element method developed, based on multi-scale multi-physics approach, was employed by Manta et al. [31], in order to analyze the influence of the potential barrier, tunneling resistance and filler shape on the percolation threshold and the electrical conductivity of graphene-polymer composites. Fang et al. [32], reported on a Monte-Carlo equipotential approximation and tunneling

conductance method, used to compute the electrical conductivity of carbon-nanotube reinforced polymer. Vas and Thomas [6], studied the behaviors of various fillers and matrix parameters variation effects on the percolation threshold and the electrical conductivity of carbon-nanotube reinforced polymer, by using the Monte Carlo approach. The lack of proper quantization of the filler morphology, inconsistency of theoretical results with experimental measurements and the omission of interaction effects, are some of the problems identified in the existing models.

In this study, an analytical model that can be deployed into a simulation tool for the optimization of parameters, the calculation of electrical conductivity and the design of polymer-composites for devices applications, has been developed. The model is based on a simple-sum approach. Percolation threshold and the electrical conductivity of polymer-composite were studied by subjecting the model developed into different ranges of parameter variations. The parameters are: (i) electrical conductivity of graphene, (ii) potential barrier, (iii) interfacial thickness and (iv) the electrical conductivity of the polymer in question. The model was used primarily to study the electrical conductivity characteristic of graphene-loaded PPy. Moreover, the results of the model were examined and validated by three experimental measurements [33–35]. It is evident that this analytical model, in conjunction with the simple-sum method, can be applied to predict the electrical conductivity of polymer-composites of any filler type and other variable parameters.

2. Simulation details

Numerical/analytical simulation of this study is divided into five parts–(i) statistical characterization of the particle length and diameter, by using the Weibull distribution, (ii) development of the interfacial conductance of the composite, (iii) computing the tunneling conductance due to the quantum effect of electrons, (iv) computing the effective conductance of the electrical circuit representation of the RVE, by applying potential difference and (v) computing the electrical conductivity of the composites by considering the potential barrier, PPy conductivity, interfacial thickness and the filler conductivity.

2.1. Statistical characterization of fillers length and diameter

The reliability and the analysis of the experimentally-derived morphology of graphene is performed, by using the Weibull distribution function [36]. If the probability density function, ϕ, of a random variable, η, having parameters, ε and ϱ, is as presented in Eq. (1), then, the distribution fitting is a 2-parameter Weibull distribution [37–39].

$$\xi(\eta;\varepsilon,\varrho)=\begin{cases}\chi\eta^{\varepsilon-1}e^{-\left(\frac{\eta}{\varrho}\right)^{\varepsilon}} & \eta\geq 0\\ 0 & \eta<0\end{cases} \tag{1}$$

where ε and ϱ, are the scale and shape parameters of the 2-parameter Weibull distribution, χ is a constant, which is equal to $\left(\frac{\varepsilon}{\varrho^{\varepsilon}}\right)$. The integral of Eq. (1), is the cumulative distribution function, C_f, of the random variables [40].

$$C_f(\eta;\varepsilon,\varrho)=\int_0^{\infty}\chi\eta^{\varepsilon-1}e^{-\left(\frac{\eta}{\varrho}\right)^{\varepsilon}}d\eta=\begin{cases}1-e^{-\left(\frac{\eta}{\varrho}\right)^{\varepsilon}} & \eta\geq 0\\ 0 & \eta<0\end{cases} \tag{2}$$

The linearized [28,41] form of Eq. (2), is presented in Eq. (3).

$$\mathrm{In}\left(-\mathrm{In}\left(1-C_f(\eta)\right)\right)=\mathrm{In}\left(\frac{\eta}{\varrho}\right)^{\varepsilon}=\varepsilon\mathrm{In}(\eta)-\varepsilon\mathrm{In}(\varrho) \tag{3}$$

The linear (straight-line) equation (Eq. (3)) can be presented as shown in Eq. (4).

$$N=m_1P+m_0+E \tag{4}$$

Assuming $N=\mathrm{In}(-\mathrm{In}(1-C_f(\eta)))$, $m_1=\varepsilon$, $P=In(\eta)$, *and* $m_0=-\varepsilon In(\varrho)$, the least square solution of Eq. (4), yields the Weibull parameters.

$$\sum_{n=1}^{N}E^2=E(m_1,\,m_0)=\sum_{n=1}^{N}(N_n-m_1P-m_0)^2 \tag{5}$$

Differentiating Eq. (5) and setting it to zero [42] yields:

$$\frac{\partial(m_1,\,m_0)}{\partial m_1}=\sum_{n=1}^{N}2(N_n-m_1P_n-m_0)P_n=0 \tag{6}$$

$$\frac{\partial(m_1,\,m_0)}{\partial m_1}=\sum_{n=1}^{N}2(N_n-m_1P_n-m_0)=0 \tag{7}$$

The matrix representation of Eqs. (6) and (7), is given in Eq. (8).

$$\sum_{n=1}^{N}\begin{pmatrix}N_nP_n\\ N_n\end{pmatrix}=\sum_{n=1}^{N}\begin{pmatrix}P_n^2 & P_n\\ P_n & 1\end{pmatrix}\begin{pmatrix}m_1\\ m_0\end{pmatrix} \tag{8}$$

where:

$$m_1=\frac{N\sum_{n=1}^{N}N_nP_n-\left(\sum_{n=1}^{N}P_n\right)\left(\sum_{n=1}^{N}N_n\right)}{N\sum_{n=1}^{N}P_n^2-\left(\sum_{n=1}^{N}P_n\right)^2} \tag{9}$$

$$m_0=\frac{\left(\sum_{n=1}^{N}P_n^2\right)\left(\sum_{n=1}^{N}N_n\right)-\left(\sum_{n=1}^{N}N_nP_n\right)\left(\sum_{n=1}^{N}P_n\right)}{N\sum_{n=1}^{N}P_n^2-\left(\sum_{n=1}^{N}P_n\right)^2} \tag{10}$$

From Eqs. (2)–(8), the Weibull parameters are represented as:

$$\varepsilon=m_1,\ and\ \varrho=exp^{-\left(\frac{m_0}{\varepsilon}\right)} \tag{11}$$

By using the Weibull distribution function, (WbDF), the sizes of the fillers are, characterized. The choice of the Weibull distribution function to characterize the parameters follows the fact that it gives a reasonable distribution of the nanomaterials sizes than other distribution fitting methods [28].

2.2. The conductance models

The electrical conductivity of polymer-composites depends on several factors, *viz:* morphologies of the fillers and the polymers, volume fractions, aspect ratio, interfacial and the

tunneling conductance, initial conductivity of the filler and polymers and many others. An analysis of the interfacial effects, alongside with other parameters, on the properties of polymer-composites, is vital in predicting the electrical conductivity of polymer composites. Several authors [29,43,44] have stated that by evaluating the electrical conductivity of polymer composites without considering the interfacial effects on the overall properties of polymer composites, will inaccurately estimate the percolation threshold of the composites. As shown in Fig. 1, the filler, dispersed randomly in the PPy, is enclosed by a thin interfacial layer. Fig. 2 is the electrical resistance network of the RVE system of Fig. 3. The network consists of the interfacial, intrinsic and tunneling conductance of the fillers. By taking the effect of the interfacial layer into consideration, the effective resistivity of a unit cell of the filler, along with the *x* and *z* directions, can be predicted by using the Kirchhoff's current law [45], to demystify the circuit of Fig. 2. In this study, the effect of the thickness of the non-chemical interaction of the filler with the polymer is segmented into three sections, along the *x*-direction as: G_x^l, G_x^r, and G_x^h, where G_x^l and G_x^r are the left and right sections of the polymer-filler interphase, G_x^h is the filler effect on the hollow interphase. In addition, the conductance in the transverse direction, is sectionalized into three groups, as: G_y^l, G_y^r and G_y^h, where G_y^l and G_y^r are the top and bottom sections, G_y^h is the hollow section of the fillers.

2.2.1. *The intrinsic conductance and interfacial effect models*

As shown in Figs. 1 and 3, the conductance along the longitudinal, i.e., *x*-direction, is the sum of the conductance: G_x^l, G_x^r and G_x^h. For the interfacial length, I, filler length, ϑ and thickness, β, the cross-sectional area (C_{SAx}) of the interface at the left section, is approximated by Eq. (12).

$$C_{SAx} = (\vartheta + 2I)^2 \tag{12}$$

The conductance, measured to the left of the interface, is given by:

$$G_x^l = \frac{\sigma_i C_{SAx}}{I} \tag{13}$$

where σ_i is the interfacial electrical conductivity, *x* is the index in the longitudinal direction and G_x^l is the conductance, measured to the left. The conductance, G_x^h, at the hollow, is a parallel connection of the conductance of the filler and the interfacial conductance experienced at the hollow, i.e.,

$$G_x^h = G_{ix}^h + G_{fx}^h \tag{14}$$

where the $G_{ix}^h = \frac{\sigma_{ix}(C_{SAx} - \vartheta^2)}{\beta}$, $G_{fx}^h = \frac{\sigma_{fx}\vartheta^2}{\beta}$ and σ_{ix} is the electrical conductivity of the fillers at the interface and σ_{fx} is the electrical conductivity of filler. The parallel conductance value of the interfacial (G_{ix}^h) and the filler (G_{fx}^h), is given by Eq. (15).

$$G_x^h = \frac{\sigma_{fx}\vartheta^2 + \sigma_{ix}(C_{SAx} - \vartheta^2)}{\beta} \tag{15}$$

From Eq. (15), the electrical conductivity of the composite at the hollow, is given as:

$$\sigma_{holx} = \frac{G_x^h \beta}{C_{SAx}} = = \frac{\sigma_{fx}\vartheta^2 + \sigma_{ix}(C_{SAx} - \vartheta^2)}{C_{SAx}} \tag{16}$$

Referring to Fig. 1, the conductance at both the left and right, are equal. Therefore, the total electrical resistance of the composite in the longitudinal direction, is:

$$R_x^T = 2R_x^l + R_x^h = \frac{2I}{\sigma_i C_{SAx}} + \frac{\beta}{\sigma_{holx} C_{SAx}} = \frac{\beta + 2I}{\sigma_x^T C_{SAx}} \tag{17}$$

Eq. (17) follows the fact that the total electrical conductivity, σ_x^T, due to interfacial effect, along the *x*-direction can be given as:

$$\sigma_x^T = \frac{\beta + 2I}{\left(\frac{2I}{\sigma_i C_{SAx}} + \frac{\beta}{\sigma_{holx} C_{SAx}}\right) C_{SAx}} = \frac{\sigma_i \sigma_{holx}(\beta + 2I)}{2I\sigma_{holx} + \beta\sigma_i} \tag{18}$$

The interfacial conductance of the system along the z-direction is segmented into three regions, namely: the top, hollow and bottom as: G_z^l, G_z^r and G_z^h. As shown in Fig. 1, the cross-sectional area of the interfacial layer at the top is:

$$C_{SAz} = (\vartheta + 2I)(\beta + 2I) \tag{19}$$

By considering the length, I, of the layer, the conductance, G_z^l, is as presented in Eq. (20).

$$G_z^l = \frac{\sigma_i C_{SAz}}{I} \tag{20}$$

The hollow segment has length, ϑ and side, β, therefore, the conductance due to the filler is:

$$G_{fz}^h = \frac{\sigma_{fz}\vartheta\beta}{\vartheta} \tag{21}$$

and the conductance due to the interfacial layer is:

$$G_{iz}^h = \frac{\sigma_i(C_{SAz} - \vartheta\beta)}{\vartheta} \tag{22}$$

Consequently, the effective conductance at the hollow is:

$$G_z^h = \frac{\sigma_{fz}\vartheta\beta + \sigma_i(C_{SAz} - \vartheta\beta)}{\vartheta} \tag{23}$$

and the electrical conductivity is:

$$\sigma_{holz} = \frac{G_z^h \vartheta}{C_{SAz}} = \frac{\sigma_{fz}\vartheta\beta + \sigma_i(C_{SAz} - \vartheta\beta)}{C_{SAz}} \tag{24}$$

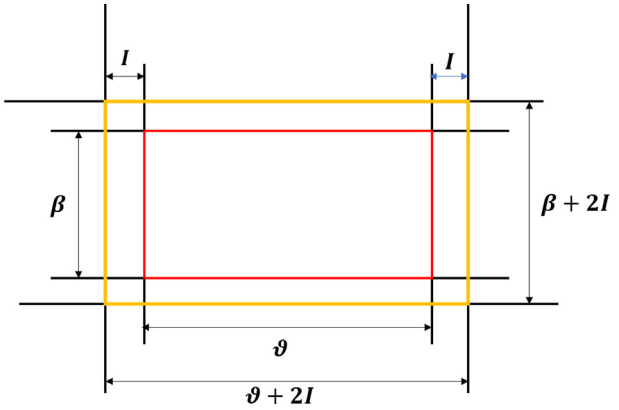

Fig. 1 – A schematic embedded view of a unit cell of filler, surrounded with an interphase layer of thickness.*I*

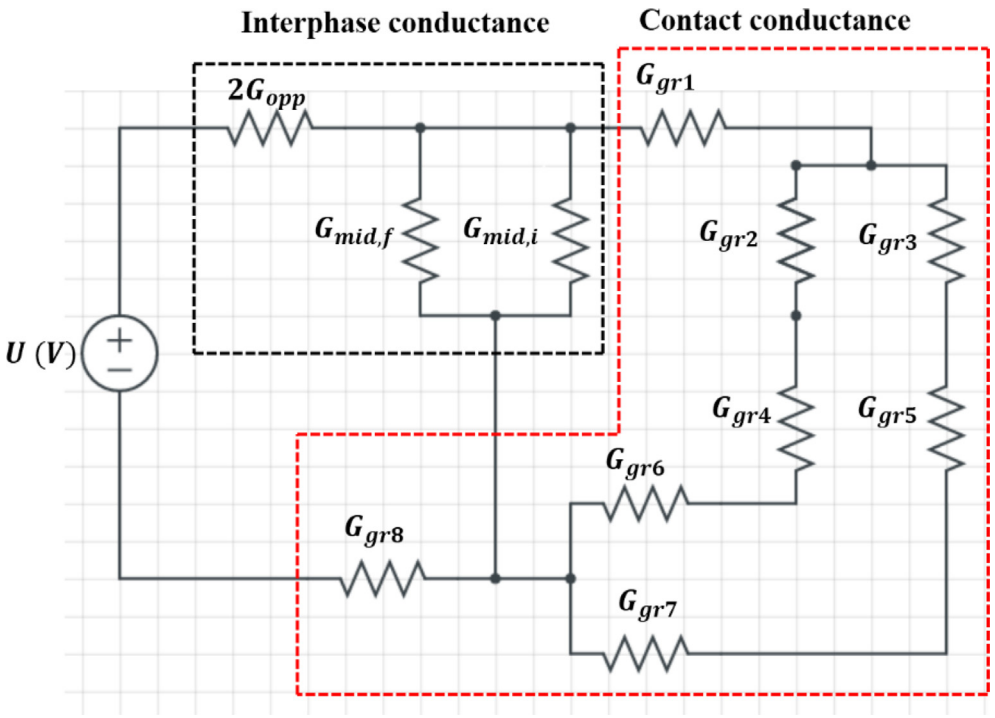

Fig. 2 – The equivalent interfacial and tunneling conductance circuit of graphene in the RVE of Fig. 3 below (G_{opp} is the sides conductance, $G_{mid,f}$ and $G_{mid,i}$ are the conductances of the filler and the interface at the middle and $G_{gr,ith}$ are the tunneling conductance, with indices 1, 2, 3, ... 8).

In the z-direction, the overall resistance due to the interfacial effect, is give as in Eq. (25).

$$R_z^T = 2R_z^l + R_z^h = \frac{2I}{\sigma_i C_{SAz}} + \frac{\vartheta}{\sigma_{holz} C_{SAz}} = \frac{\vartheta + 2I}{\sigma_z^T C_{SAz}} \tag{25}$$

Therefore, along the z-direction, the electrical conductivity of the individual filler is:

$$\sigma_z^T = \frac{\vartheta + 2I}{\left(\frac{2I}{\sigma_i C_{SAz}} + \frac{\vartheta}{\sigma_{holz} C_{SAz}}\right) C_{SAz}} = \frac{\sigma_i \sigma_{holz}(\vartheta + 2I)}{\vartheta \sigma_i + 2I\sigma_{holz}} \tag{26}$$

Having considered the effect of the interfacial interaction of the particles, the intrinsic conductivity of the composite in the longitudinal and transverse directions, are:

$$G_x^i = \frac{\vartheta^2 \pi \sigma_x^T}{4\beta} \tag{27}$$

and

$$G_z^i = \frac{\beta^2 \pi \sigma_z^T}{4\vartheta} \tag{28}$$

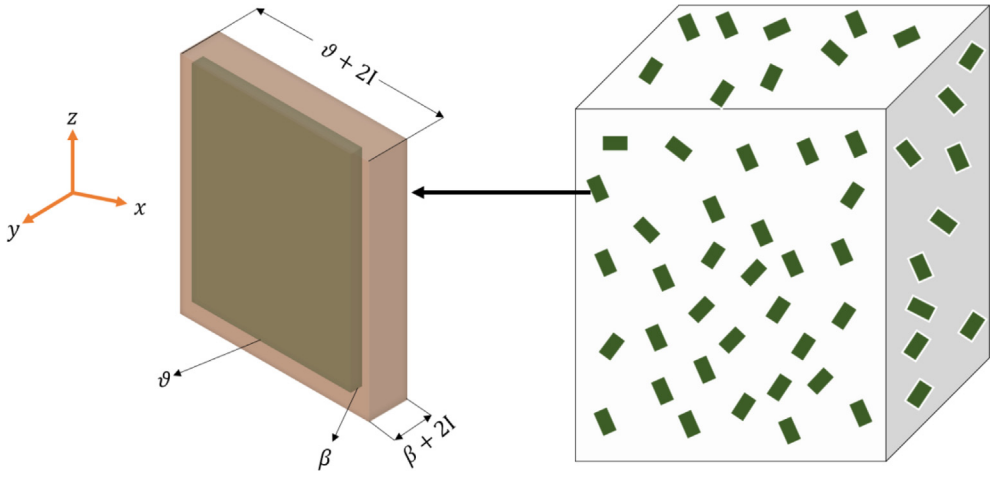

Fig. 3 – The random distribution of graphene fillers in polypyrrole, showing the length and thickness of the filler (ϑ, β); I is the barrier thickness, in the representative volume element (RVE).

2.2.2. The tunneling conductance model

For conduction to place in a polymer-composite, the neighboring filler must interact and make contact with each other; this physical contact is known as electron tunneling. The tunneling effect results in the escape of electrons, which constitutes the total electrical conductivity of the composites. When a tunneling distance exists between the fillers, in a polymer-composite electrical network, the semiconducting polymer becomes a conducting material when the distance is relatively small. The distance between the nanoparticles is within a range of nanometers; therefore, tunneling may occur, and since tunneling current is an exponential function of the distance between the neighboring particles, the tunneling or contact resistance can be assumed to occur between two nearest particles [19,46]. The thickness of PPy between a pair of fillers is an indicator that the effect of tunneling in the composite cannot be ignored [32,47,48].

Recall, at temperatures below or equal zero (0 K), electrons reside in the lowest energy level of a system. However, as the temperature increases above zero, both the conduction and valence band contribute to electron tunneling. As such, the equivalent conduction channels [17,18] can be given as:

$$N^{ch} = \sum_{Bands} \frac{1}{\left(exp^{\left(E_h - E_F / kT \right)} + 1 \right)} \tag{29}$$

where E_h is the band with the highest energy, E_F is the Fermi energy level, kT is the thermal energy. The probability of electrons transiting through the PPy barriers between filler can be calculated [32] by:

$$\alpha = exp^{\left(-\frac{m}{\phi} \right)} \tag{30}$$

where ϕ is the parameter relating to the tunneling distance, and it is given [31] as:

$$\phi = \frac{h}{4\pi\sqrt{2m_q\omega}} \tag{31}$$

and m is $2I$ [49]. The total tunneling conductance is proportional to the probability of electron transmission between the matrix and the fillers. Hence, Eq. (32) is the effective tunneling conductance (G_{tnl}) of the composites.

$$G_{tnl} = q_0 N^{ch} \phi \tag{32}$$

where q_0 [50], is the quantum conductance $\left(q_0 = \frac{2e^2}{h} \right)$. Rearranging Eqs. (29)–(32), the total tunneling conductance is given as:

$$G_{tnl} = \frac{2e^2 N^{ch}}{h} exp^{\left(-\frac{4\pi T\sqrt{2m_q\omega}}{h} \right)} \tag{33}$$

Herein, ω is the potential energy barrier, h is the Planck constant, e is the electron charge, m_q is the mass of electron. The number of conducting channels per graphene layer was approximated by Naeemi and Meindl [18]:

$$N^{ch} = a.D + b. \tag{34}$$

where $a. = 0.0612\ nm^{-1}$ and $b. = 0.425$ [18]. In this study, D is taken as the diameter of the filler.

2.2.3. The effective conductance of PPy-graphene composite

Several authors [6,51,52], have reported that on the total conductance of a polymer-composite, as provided, is the sum of the intrinsic and the tunneling conductance of composite. Therefore, along the longitudinal direction, the conductance is:

$$G_{xT} = \frac{\vartheta^2 \pi \sigma_x^T}{4\beta} + \frac{2e^2(a.\vartheta + b.)}{h} exp^{\left(-\frac{4\pi T\sqrt{2m_q\omega}}{h} \right)} \tag{35}$$

and along the transverse direction, the conductance is:

$$G_{yT} = \frac{\beta^2 \pi \sigma_z^T}{4\vartheta} + \frac{2e^2(a.\beta + b.)}{h} exp^{\left(-\frac{4\pi T\sqrt{2m_q\omega}}{h} \right)} \tag{36}$$

Finally, the electrical conductivity of the composite, due to interface, intrinsic and contact resistance, is:

$$\sigma_R = \frac{4l_j G_{jT}}{\pi D_j^2} \tag{37}$$

where j is the index of direction.

2.3. The electrical conductivity predictive model

The statistical percolation law of Kirkpatrick [53], is an empirical power law of polymer-composite electrical conductivity, from a predictive model, as presented by:

$$\sigma_c = \sigma_0 (\upsilon - \upsilon_c)^t \quad for\ \upsilon > \upsilon_c \tag{38}$$

where υ_c is the threshold concentration, υ is the filler concentration, σ_0 is the initial conductivity of the matrix and σ_c is the composite conductivity. The empirical power-law model, though effective, however, shows, the experimental dependence of the exponent, t, renders it less accurate and difficult to ascertain its significance [16,54]. In this study, based on the analytical modelling of the composite conductance, a simple-sum method approach, is proposed to predict the electrical conductivity of graphene-PPy composite and it is given by:

$$\sigma_c = \psi(\sigma_g + \sigma_R) + \sigma_m \tag{39}$$

The parameter, ψ [49], is a function, which depends on the volume fraction of the filler and the percolation threshold of the composite; σ_g is the conductivity of the filler and σ_m is the matrix conductivity.

3. Experimentation

The PPy powder was obtained from Sigma Aldrich, South Africa. The PPy (code no: 530573-25G), has already been doped with sulfonic acid, having a 30 vol% loading of carbon black, raising its electrical conductivity to 30 S/cm. The graphene used as a conductive filler was purchased from Sigma Aldrich, South Africa. The product description reads the morphology as follows: 5 μm diameter, the surface area of between 50 and 80 m^2/g, bulk density of 0.03–0.1 g/cm^3, the average thickness

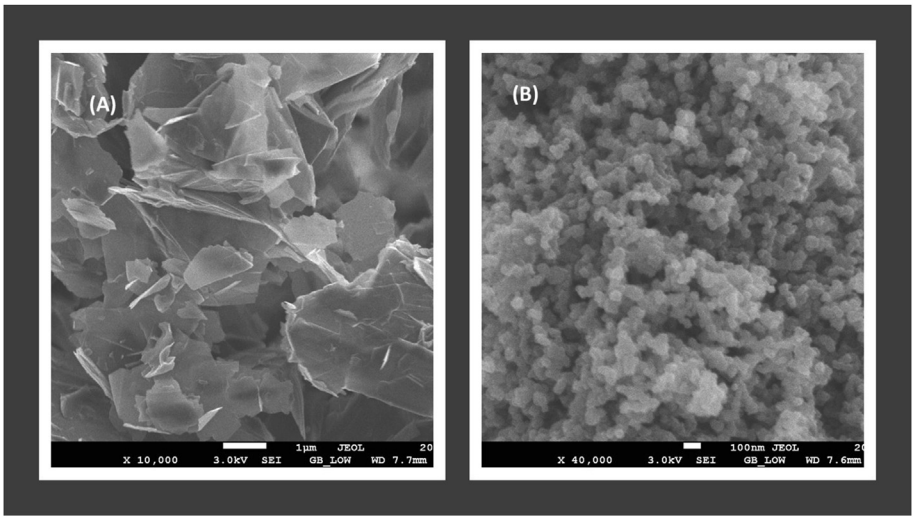

Fig. 4 – Scanning electron microscopic graph of (a) Graphene and (b) Polypyrrole.

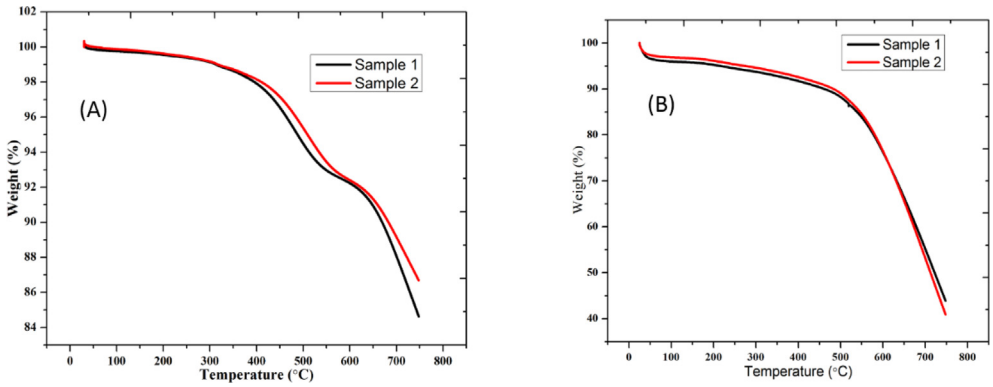

Fig. 5 – TGA curve of (a) Graphene and (b) Polypyrrole.

of 15 nm, less than 0.01 oxygen content and residual acid content of fewer than 0.5 wt%.

The thermal stability study of the materials was investigated under nitrogen atmosphere by using a TGA 5500 (1200 °C ambient temperature, 0.1–500 °C/min heating rate (linear), >1600 °C heating rate (ballistic) and a sample weight capacity of 1000 mg). The morphology of the particles was analyzed by using the scanning electron microscope equipment, SEM (Zeiss, Berlin, Germany). Furthermore, the XRD pattern was recorded by using X-ray diffractometer with Cu-K_α radiation (XPert Pro X-Ray Diffractometer Panalytical, Eindhoven, The Netherlands).

Briefly, from the analysis of the materials morphologies, the calculated average diameter, length and area of the graphene, are: 2.5 μm, 500 nm, and 23,500 nm^2, respectively. The SEM images of graphene and PPy are shown in Fig. 4. Moreover, the average diameter, area and length of PPy, are: 57.85 nm, 21,000 nm and 90 nm, respectively. Fig. 5 gives the thermogravimetric analysis of the graphene and the PPy for the two different samples. Fig. 5(a) shows that the graphene has very low decomposition between 30.20 °C until 316.30 °C due to the evaporation of the adsorption water. However, a sharp decomposition begins at 414.40 °C until 574.90 °C, and the final decomposition occurs between 574.90 and 750 °C. That is, the entire mass of the graphene would be lost at temperatures between 574.90 and 750 °C [55]. Fig. 5(b) shows that the PPy experienced a very noticeable decomposition at 25 °C until 41.4 °C and continuous degradation of the material begins at 190 °C. Furthermore, the X-ray diffraction patterns of graphene and PPy, are shown in Fig. 6. The PPy has broad peaks at $2\theta = 11.20^{\circ}$, 25.00° and 41°. The identification of these broad peaks is evidence of the amorphous nature of the material. Moreso, the long narrow peak of graphene at 26.20°, is an indication of the crystalline nature of the material and the presence of carbon.

The graphene-PPy composite was prepared by *in-situ* polymerization. Without further purification of the chemicals used, graphene was dispersed in 50 ml of deionized water, by ultrasonication for 30 min. Afterwards, a measured quantity of Py was added to a mixture of 1:3 (30 ml) deionize water and ethanol. The solution of the Py was gently added to the dispersed graphene and sonicated for 30 min. Moreso, a

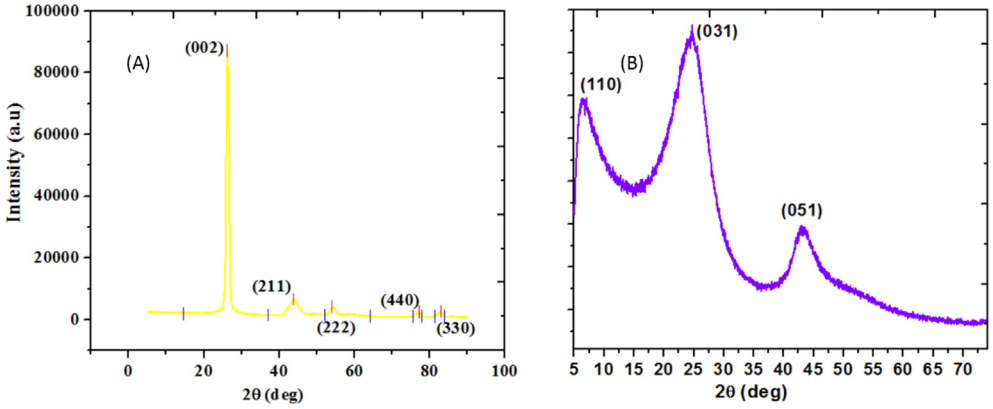

Fig. 6 – XRD diffractogram of (a) Graphene and (b) Polypyrrole.

weighed amount of ferric chloride, was added to a 1:2 mixture of deionized water and hydrochloric acid and the solution was sonicated for 30 min. In addition, a solution of the ferrous chloride was added, dropwise to the graphene-Py and it was rigorously stirred for over 12 h. The composite obtained was allowed to dry in an oven, at 75 °C. The uniform distribution of graphene in graphene-PPy composite was investigated with a SEM and the micrographs obtained are shown in Fig. 7. As shown in Fig. 7, the surface of the graphene was successfully covered by the PPy. The agglomerate of PPy on the surface of the graphene sheets, confirms the van der Waals force and $\pi-\pi$ interactions of the materials [56]. In our next study, the critical experimental analysis of graphene-polypyrrole and a hybrid of graphene with other 2-dimensional materials, for energy storage advantages, will be discussed. In the present study, our focus is to discuss the analytical simulation of the graphene-PPy composite.

The materials morphologies were quantized by using available software and the data, plotted as histograms, as shown in Figs. 8 and 9. The shapes of the histograms (Figs. 8 and 9) suggest to some degree, the accuracy that the Weibull distribution could characterize the materials data; this argument is in agreement with the work of Wang et al. [28].

4. Results and discussion

In this section, the analytical model developed, is verified and validated, by applying it to predict the electrical conductivity of: (i) carbon black, loaded on ethylene-propylene diene monomer, (ii) graphene nanoplatelets, loaded on polymerized cyclic butylene terephthalate and (iii) graphene nanoparticles, loaded epoxy resin.

4.1. *Length and distribution*

The structure, orientation angles, dispersion and interfacing effect, load sharing and mobility of electrons between the matrix and the filler, are somewhat difficult to consider when creating models to predict the properties of polymer-composites. In order to reduce this complex effect, it is necessary to characterize the random distribution of filler, size and length in order to be able to present accurate models that will predict the electrical properties of polymer-composites [28,57,58]. The theoretical distribution of graphene size plotted against the experimental data, gives the Weibull probability distribution plot, as shown in Figs. 10 and 11.

Figs. 10 and 11 show that the theoretical distributions form of approximate points with the extreme value curve. In this study, the Weibull distribution was used to describe the lengths and diameters of the graphene nanoparticles in order to predict the electrical conductivity of the graphene-PPy composite. Presented in Table 1 are the estimated parameters for the Weibull distribution function.

4.2. *Model validation*

The model was validated by comparing the predicted percolation threshold and the electrical conductivity of the different polymer-composites with experimental measurements, sourced from the available literature. Ghosh and Chakrabarti [35], presented the experimental data on the conducting carbon black-filled ethylene/propylene diene monomer. The two procedural methods employed by Ghosh and Chakrabarti, which are the: compounding of the polymer and filler at a temperature of 75 ± 2 °C and the vulcanization of the composite in a compressing moulding machine at a temperature of 160 ± 2 °C, under a pressure of 80 kgf.cm^{-2}. As reported by Ghosh and Chakrabarti, the particle diameter was 30 μm and the length was in the range of between 1.5 – 2.0 μm [59]. Fig. 12a shows the comparison of the experimental results with the results of the model of Eq. (39). Fig. 12a clearly shows that there is a correlation between the experimental results and the modelled results. The Montel Carlo simulation results, presented by Vas and Thomas [6] on the composite, is in agreement with the results of the model developed in this study.

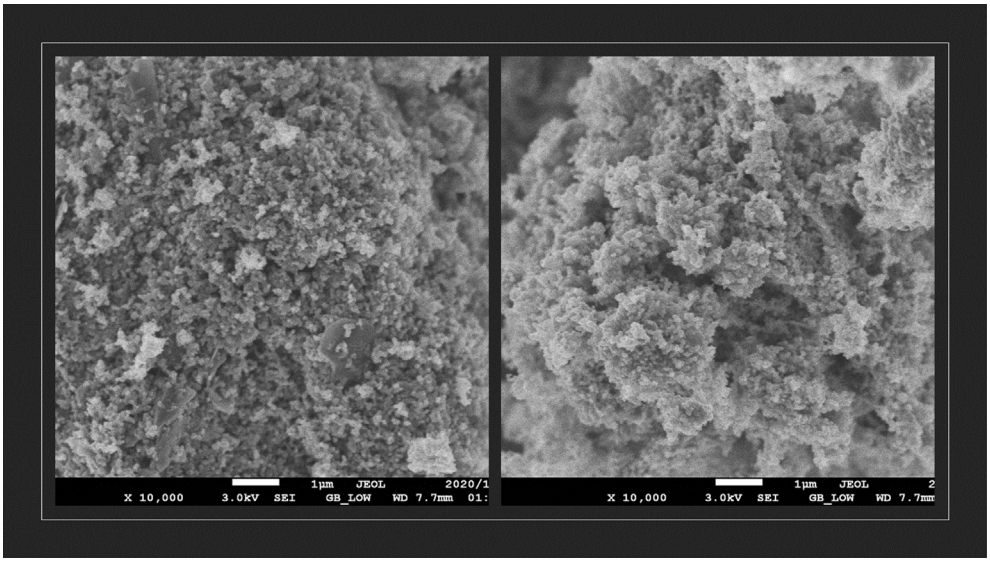

Fig. 7 – Scanning electron micrograph of graphene-polypyrrole composite at two different magnifications.

Another set of data used in the validation process of the model developed in this work was presented by Kim et al. [34]. Kim et al. [34], carried out the experimental and analytical investigations of the electrical percolation of graphene nanoplatelets-loaded polymerized cyclic butylene terephthalate. The graphene had a thickness and diameter of 6 nm and 5 μm, respectively. The initial electrical conductivity of the polymer was 8.5×10^{-14} S/m [60]; other parameters involved in the calculations, were: 1.57 nm graphene length and potential barrier of 2.1 eV [6]. Figure 12b is the comparative results of Kim et al. experimental work [34] and the present study. Fig. 12b shows that there is close agreement between the percolation threshold of the experimental results and the model developed in the present study. The result of this study is also in agreement with the investigation of Fang et al., [46].

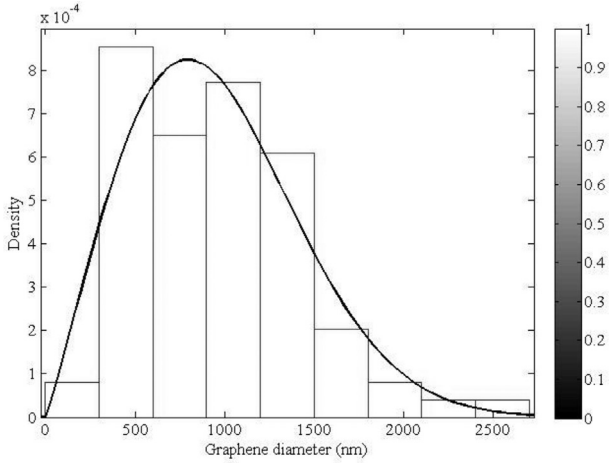

Fig. 8 – The histogram of the graphene dispersed diameter (nm).

In order to further validate the model developed, the experimental results of the study conducted by Hashjin et al., [33] was compared with the model results developed in this study. Hashjin et al. [33], studied the loading effects of graphene on epoxy coatings by dispersing graphene in chloroform, followed by cooling and the gradual mixing of the epoxy resin with the graphene solution. The diameter, thickness and conductivity of the graphene that are required to control the property of the epoxy were: 10 μm, 1.2 nm and 473 S/m [33], respectively; the potential energy barrier was set at 10 eV, and the initial conductivity of the polymer was given as 7.17×10^{-14} (S/m) [33]. Figure 12c displays the comparison results of the model with the experimental data. From Fig. 12c, it can be seen that the model results, aligned closely with the experimental results and analytical results of Mamunya and Kirkpatrick and Zallen, as shown by Hashjin et al. [33].

4.3. *Parameters variation effects*

The quantized length and diameter of graphene, by using the Weibull distribution, as shown in Figs. 8 and 9 and Table 1, were used in the calculation of the electrical conductivity of the graphene-PPy composite. The PPy and the **graphene, have initial conductivities** of 30 S/cm and 10^3 **S/m, respectively.** The potential energy barriers, interfacial thickness, filler conductivity, were varied in order to observe their effects on the effective conductivity of the composites. In addition, the effects of the intrinsic PPy electrical conductivity on the total conductivity of the composites were observed.

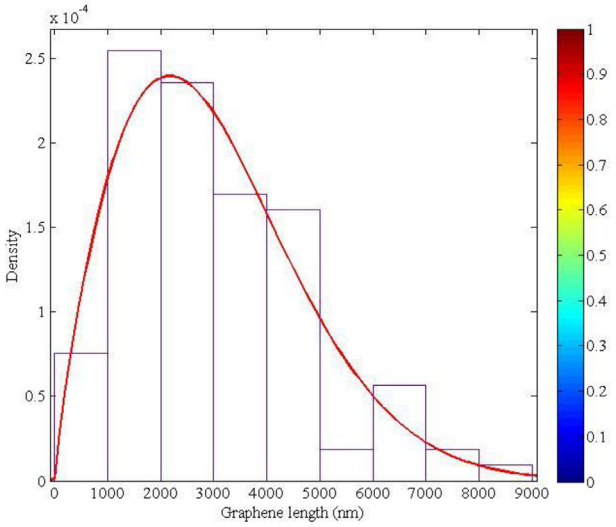

Fig. 9 – The histogram of graphene dispersed length (nm).

4.3.1. *Graphene conductivity variation effect on the composite*

From Eq. (39), it can be deduced that the electrical conductivity of a composite, depends on the electrical conductivity of the filler, intrinsic, tunneling and interface conductance of the composite. For a 1.2 *eV* potential energy barrier, 1 *nm* interface thickness and 30 *S/cm* PPy conductivity, **the effects of graphene conductivity were observed to be in the range of between** 10 **to** 10^6 **S/m**. As shown in Fig. 13, the composite conductivity is equal to the PPy conductivity, when the weight fraction equals zero. Moreover, as the filler conductivity increases, the composite experienced a constant percolation threshold at a weight fraction of 0.001(*wt*) for all the conductivities. Furthermore, for the filler conductivity range of between 10^2 to 10^6 S/m, the electrical conductivity of the composite changes from 3000 to 3003.5 *S/m*, for a total weight fraction of 0.03 (*wt*). From these results, it can be affirmed that the effective conductivity of the composites, is a function of the filler conductivity and the weight fraction of the filler. The results of this model agreed with the work of Vas and Thomas [6].

4.3.2. *Potential barrier effect*

Recall, the insulating layer of polymer is the barrier that limits the electrical conductivity of polymer composites. Therefore, the energy, which must create conduction in the composite, must be greater than or equal to the polymer insulating barrier energy [61]. Hence, in this study, the effect of the potential energy barrier in the conductance of graphene-PPy composite is investigated, by using PPy having a conductivity value of 30 *S/cm* and a filler with a conductivity value of 10^5 *S/m*, a 2 *nm* interfacial thickness, the quantized length and diameter. The barrier potential is set to a range of between 1 – 7*eV* [46]. The results obtained are, as shown in Fig. 14. From Fig. 14, it can be seen that the energy barrier potential has a direct effect on the conductivity of the composite, that is: the higher the barrier potential, the lower the electrical conductivity of the composite. Moreover, below the percolation threshold, the electrical conductivity of the composite remained independent of the potential barrier; but its influence on the electrical conductivity above **the** percolation threshold is perceptible. These results agree with the analytical results of Fang et al. [32] and other authors [44,62].

4.3.3. *Interfacial thickness effect*

The interfacial effect of the composite is investigated by setting the potential barrier at 2 *eV*, filler conductivity at 10^5 *S/m*, polymer conductivity at 30 *S/cm*; the length and diameter, remained as quantized. The interface thickness is varied between 1 and 5 *nm*. From Fig. 15, **it is observed that the thickness of the composite is inversely proportional to the percolation threshold without any significant impact on the total electrical conductivity of the composite, i.e., as the thickness increases, the composite needs a considerable amount of the volume fraction of the filler to form conducting paths**. Moreso, the electrical conductivity of the composite marginally decreases as the interfacial thickness increases. **This effect can be attributed to the fact that the interfacial thickness influences the electrons, which transit across the insulating layer of the polymer. A reduced thickness will make the composite to result in more current density**. These results agreed with literature reports [29,44,63] and the values

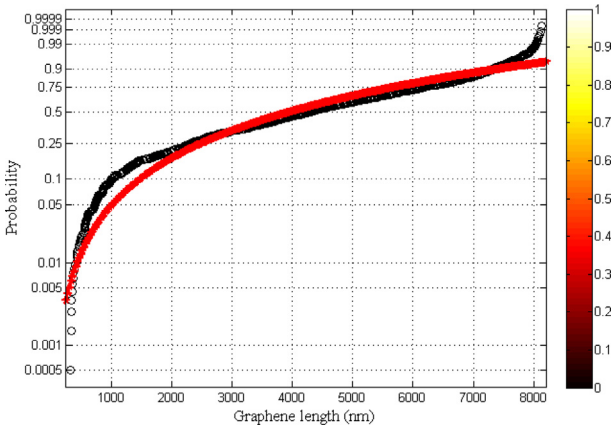

Fig. 10 – The Weibull probability plot of graphene nanoparticles lengths.

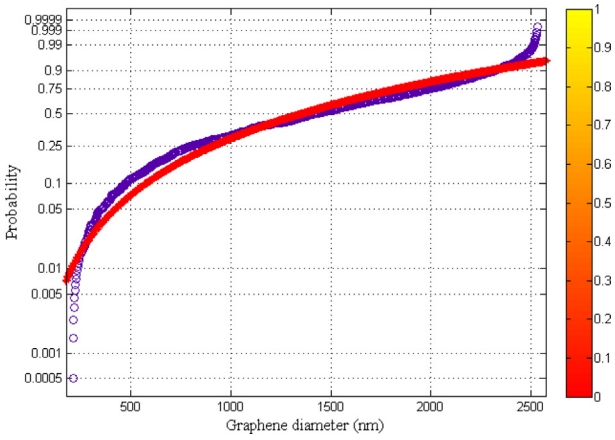

Fig. 11 – The Weibull probability plot of graphene nanoparticles diameters.

Table 1 – Weibull parameters for graphene length and diameter.

Parameter	Log Likelihood	Mean	Variance	ε	ϱ
Diameter	−7904.37	1405.89	440175	1587.31	2.2412
Length	−9123.42	4238.77	5.295E6	4778.18	1.9178

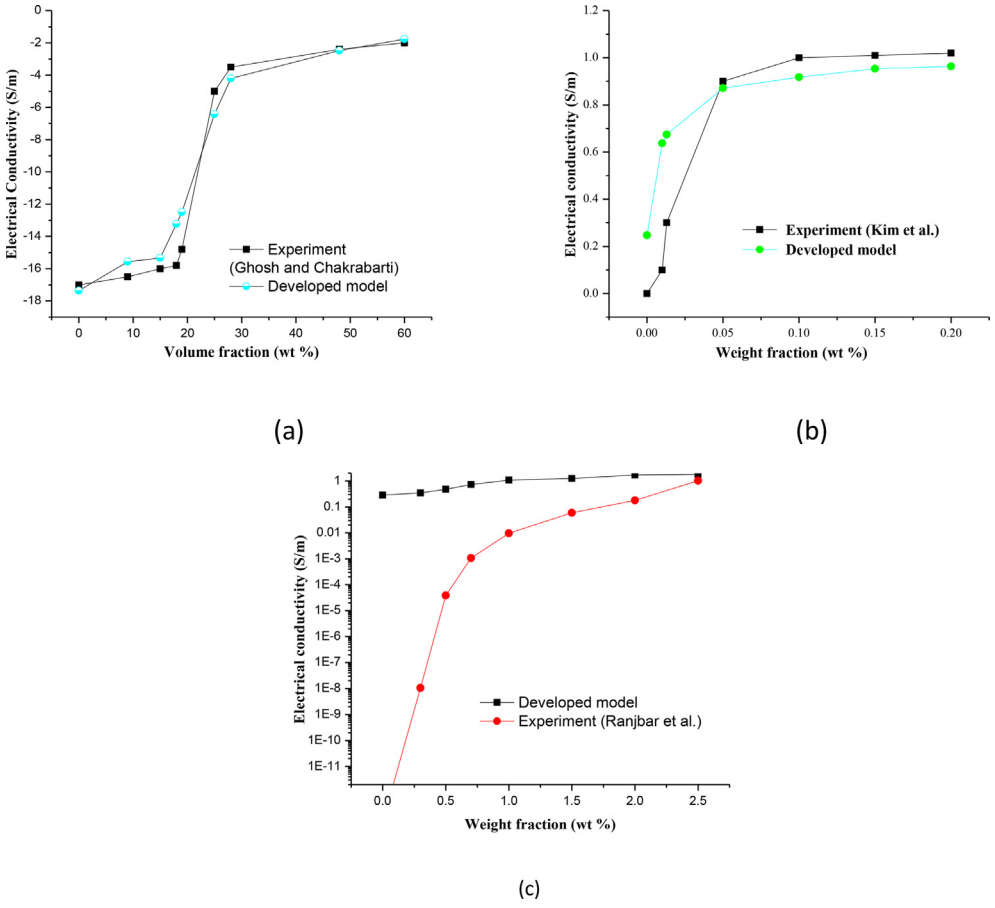

Fig. 12 – Model result versus experimental data. (a) Ghosh and Chakrabarti [35] (b) Kim et al. [34] (c) Ranjbar et al. [33].

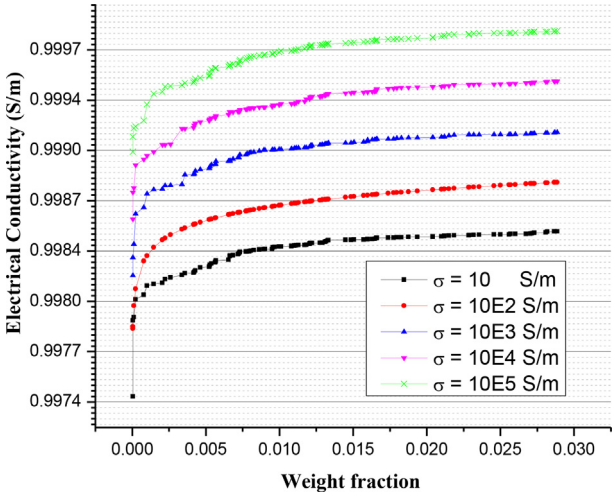

Fig. 13 – Graphene electrical conductivity effects on graphene-PPy composite.

of the thickness chosen, were in accordance to the literature [64].

4.3.4. *Effect of electrical conductivity of the matrix*

The effect of polymer conductivity is illustrated in Fig. 16. The simulation values of the parameters used are: intrinsic matrix electrical conductivity that ranges between 10^{-12} – 10^{-8} S/m, filler conductivity is 10 s/m, the potential barrier is 2 eV, the interfacial thickness is 2 nm, the quantized length and diameter. From Fig. 16, it can be seen that beyond percolation threshold, the electrical conductivity of the composite is independent of the matrix conductivity. The lowest conductivity value of the matrix requires a large weight fraction of the filler in order to bring the composite to the percolation threshold that will raise the electrical conductivity of the composite. In addition, the results show that the matrix conductivity has an influence on the total composite conductivity below the percolation threshold. Nevertheless, once the composite gains continuous conduction,

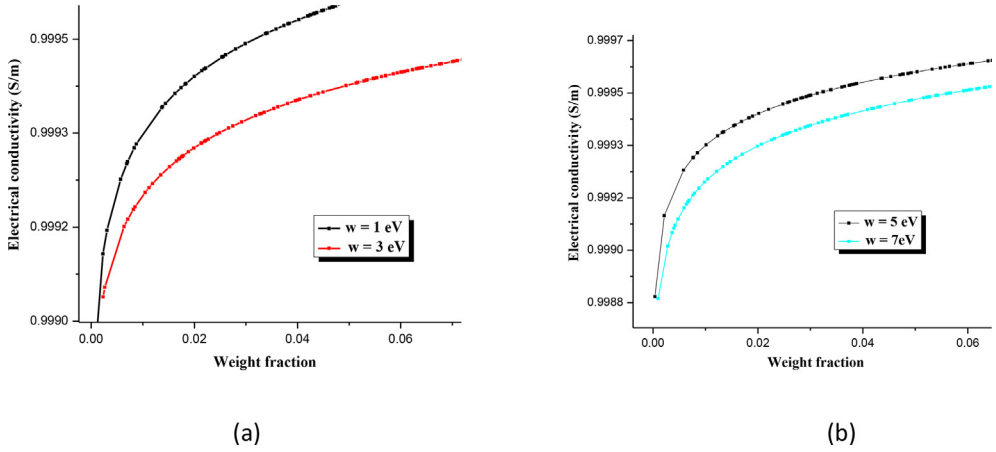

Fig. 14 – Potential barrier effects on the electrical conductivity of graphene-PPy composites (a) *w* is between 1 and 3 *eV* (b) *w* is between 5 and 7 *eV*.

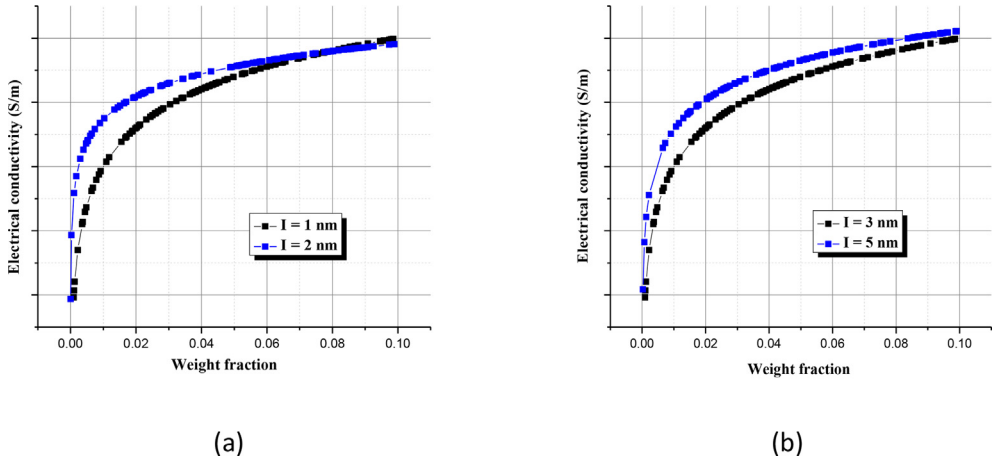

Fig. 15 – Interfacial thickness effect on the electrical conductivity of graphene-PPy composite (a) thickness varied between 1 and 2 *nm* and (b) thickness varied between 3 and 5 *nm*.

the total conductivity becomes a function of the contact and the tunneling conductance. The analytical results of several authors [29,32,46], agreed with the results of the current model.

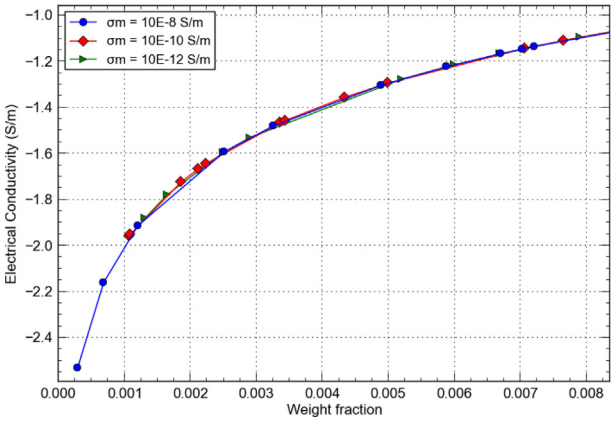

Fig. 16 – Polymer conductivity effect on the percolation and overall electrical conductivity of the composite.

5. Conclusion

Experimental characterization of graphene morphology and their statistical quantization have been carried out, by using the Weibull distribution approach. A predictive polymer-composite electrical conductivity model that incorporated the interface effect, in conjunction with a simple-sum approach, has been developed. The investigation was concerned with the evaluation of the electrical conductivity changes of graphene-polypyrrole composite, in response to interfacial thickness, polypyrrole conductivity, graphene conductivity and energy barrier. The model developed, predicted that the percolation threshold remained constant with increasing filler conductivity. In contrast, the composite effective electrical conductivity increases with increasing filler conductivity. Moreover, the model predicted the fact that

for a decreasing interfacial thickness, the percolation threshold increased and the electrical conductivity of the composite decreased. Furthermore, it was observed that the potential energy barrier, has an inverse effect on the electrical conductivity of the composite, above the percolation threshold. In addition, it was observed that the polymer-conductivity level could not dictate the effective conductivity of the composite above the percolation threshold; consequently, the polymer conductivity can only influence the effective electrical conductivity of the composite below a percolation point. More so, the statistical distribution of the filler morphology aids the accuracy of the predictive model. The results from the predictive model are in good agreement with experimental measurements, sourced from the literature [33–35]. Further studies will analytically and experimentally, investigate how the percolation threshold and the electrical conductivity of composites, affect the electrochemical devices.

Declaration of Competing Interest

The authors declare that they have no known competing financial interests or personal relationships that could have appeared to influence the work reported in this paper.

Acknowledgments

This research was supported by Tshwane University of Technology, Pretoria, South Africa. Also, to the author, SS. Ray thanks the Department of Science and Innovation and the Council for Scientific and Industrial Research, South Africa for financial support.

REFERENCES

[1] Dipojono HK, Syafitri I, Saputro AG. Immobilization of leucine on polypyrrole for biosensor applications: a density functional theory study. In: International conference on instrumentation, communication, information technology, and biomedical engineering 2009. IEEE; 2009. p. 1–3.
[2] Fulari V, Thombare J, Kadam A. Chemical oxidative polymerization and characterization of polypyrrole thin films for supercapacitor application. In: 2013 international conference on energy efficient technologies for sustainability. IEEE; 2013. p. 1068–71.
[3] Bhatt CM, Jampana N. Comparative studies on electrical properties of polypyrrole based gas sensor. In: 2011 IEEE sensors applications symposium. IEEE; 2011. p. 131–5.
[4] Folorunso O, Hamam Y, Sadiku R, Ray SS, Adekoya GJ. Investigation of graphene loaded polypyrrole for lithium-ion battery. Mater Today: Proceedings 2020. https://doi.org/10.1016/j.matpr.2020.03.522 (Article in Press).
[5] Zhang Y, Zhao Y, Konarov A, Gosselink D, Soboleski HG, Chen P. A novel nano-sulfur/polypyrrole/graphene nanocomposite cathode with a dual-layered structure for lithium rechargeable batteries. J Power Sources 2013;241:517–21.
[6] Vas JV, Thomas MJ. Monte Carlo modelling of percolation and conductivity in carbon filled polymer nanocomposites. IET Sci Meas Technol 2017;12(1):98–105.
[7] Lv W, Li Z, Deng Y, Yang Q-H, Kang F. Graphene-based materials for electrochemical energy storage devices: opportunities and challenges. Energy Storage Mater 2016;2:107–38.
[8] Garaj S, Hubbard W, Golovchenko JA. Graphene synthesis by ion implantation. Appl Phys Lett 2010;97(18):183103.
[9] Ambrosi A, Pumera M. Electrochemically exfoliated graphene and graphene oxide for energy storage and electrochemistry applications. Chem Eur J 2016;22(1):153–9.
[10] Ghorbani M, Abdizadeh H, Golobostanfard M. Reduction of graphene oxide via modified hydrothermal method. Procedia Mater Sci 2015;11:326–30.
[11] Hummers Jr WS, Offeman RE. Preparation of graphitic oxide. J Am Chem Soc 1958;80(6). 1339-1339.
[12] Yu H, Zhang B, Bulin C, Li R, Xing R. High-efficient synthesis of graphene oxide based on improved hummers method. Sci Rep 2016;6:36143.
[13] Folorunso O, Hamam Y, Sadiku R, Ray SS, Adekoya GJ. Electrical resistance control model for polypyrrole-graphene nanocomposite: energy storage applications. Mater Today Commun 2020:101699.
[14] Brownson DA, Kampouris DK, Banks CE. An overview of graphene in energy production and storage applications. J Power Sources 2011;196(11):4873–85.
[15] Alian A, Meguid S. Multiscale modeling of the coupled electromechanical behavior of multifunctional nanocomposites. Compos Struct 2019;208:826–35.
[16] Hu N, Masuda Z, Yan C, Yamamoto G, Fukunaga H, Hashida T. The electrical properties of polymer nanocomposites with carbon nanotube fillers. Nanotechnology 2008;19(21):215701.
[17] Li HJ, Lu W, Li J, Bai X, Gu C. Multichannel ballistic transport in multiwall carbon nanotubes. Phys Rev Lett 2005;95(8):086601.
[18] Naeemi A, Meindl JD. Compact physical models for multiwall carbon-nanotube interconnects. IEEE Electron Device Lett 2006;27(5):338–40.
[19] Venugopal A, Colombo L, Vogel E. Contact resistance in few and multilayer graphene devices. Appl Phys Lett 2010;96(1):013512.
[20] Yu Y, Song G, Sun L. Determinant role of tunneling resistance in electrical conductivity of polymer composites reinforced by well dispersed carbon nanotubes. J Appl Phys 2010;108(8):084319.
[21] Mamunya E, Davidenko V, Lebedev E. Effect of polymer-filler interface interactions on percolation conductivity of thermoplastics filled with carbon black. Compos Interfac 1996;4(4):169–76.
[22] Radzuan NAM, Sulong AB, Rao Somalu M. Electrical properties of extruded milled carbon fibre and polypropylene. J Compos Mater 2017;51(22):3187–95.
[23] Taipalus R, Harmia T, Zhang M, Friedrich K. The electrical conductivity of carbon-fibre-reinforced polypropylene/polyaniline complex-blends: experimental characterisation and modelling. Compos Sci Technol 2001;61(6):801–14.
[24] Weber M, Kamal MR. Estimation of the volume resistivity of electrically conductive composites. Polym Compos 1997;18(6):711–25.
[25] Folorunso O, Hamam Y, Sadiku R, Ray SS, Joseph AG. Parametric analysis of electrical conductivity of polymer-composites. Polymers 2019;11(8):1250.
[26] Taherian R. 11 developments and modeling of electrical conductivity in composites. In: Electrical conductivity in

polymer-based composites: experiments, modelling, applications; 2018. p. 297.
[27] T.-T. Le, "Probabilistic modeling of surface effects in nano-reinforced materials," Comput Mater Sci, vol. 186, p. 109987.
[28] Wang S, Liang Z, Wang B, Zhang C. Statistical characterization of single-wall carbon nanotube length distribution. Nanotechnology 2006;17(3):634.
[29] Yan K, Xue Q, Zheng Q, Hao L. The interface effect of the effective electrical conductivity of carbon nanotube composites. Nanotechnology 2007;18(25):255705.
[30] Senghor FD, Wasselynck G, Bui HK, Branchu S, Trichet D, Berthiau G. Electrical conductivity tensor modeling of stratified woven-fabric carbon fiber reinforced polymer composite materials. IEEE Trans Magn 2017;53(6):1–4.
[31] Manta A, Gresil M, Soutis C. Predictive model of graphene based polymer nanocomposites: electrical performance. Appl Compos Mater 2017;24(2):281–300.
[32] Fang C, Zhang J, Chen X, Weng GJ. A Monte Carlo model with equipotential approximation and tunneling resistance for the electrical conductivity of carbon nanotube polymer composites. Carbon 2019;146:125–38.
[33] Ranjbar Z, Yari H. Modeling of electrical conductive graphene filled epoxy coatings. Prog Org Coating 2018;125:411–9.
[34] Kim SY, Noh YJ, Yu J. Prediction and experimental validation of electrical percolation by applying a modified micromechanics model considering multiple heterogeneous inclusions. Compos Sci Technol 2015;106:156–62.
[35] Ghosh P, Chakrabarti A. Conducting carbon black filled EPDM vulcanizates: assessment of dependence of physical and mechanical properties and conducting character on variation of filler loading. Eur Polym J 2000;36(5):1043–54.
[36] Weihull W. A statistical distribution function of wide applicability. J Appl Mech 1951;18:290–3.
[37] Almalki SJ, Yuan J. A new modified Weibull distribution. Reliab Eng Syst Saf 2013;111:164–70.
[38] Bagheri S, Samani EB, Ganjali M. The generalized modified Weibull power series distribution: theory and applications. Comput Stat Data Anal 2016;94:136–60.
[39] Nassar M, Afify AZ, Dey S, Kumar D. A new extension of Weibull distribution: properties and different methods of estimation. J Comput Appl Math 2018;336:439–57.
[40] Almalki SJ, Nadarajah SJRE, Safety S. Modifications of the Weibull distribution: a review. Reliab Eng Syst Saf 2014;124:32–55.
[41] Lauer C, Schmier S, Speck T, Nickel KG. Strength-size relationships in two porous biological materials. Acta Biomater 2018;77:322–32.
[42] Lu JZ, Monlezun CJ, Wu Q, Cao QV. Fitting Weibull and lognormal distributions to medium-density fiberboard fiber and wood particle length. Wood Fiber Sci 2007;39(1):82–94.
[43] Mazaheri M, Payandehpeyman J, Khamehchi M. A developed theoretical model for effective electrical conductivity and percolation behavior of polymer-graphene nanocomposites with various exfoliated filleted nanoplatelets. Carbon 2020;169:264–75.
[44] Payandehpeyman J, Mazaheri M, Khamehchi M. Prediction of electrical conductivity of polymer-graphene nanocomposites by developing an analytical model considering interphase, tunneling and geometry effects. Compos Commun 2020:100364.
[45] Wang G, Wang C, Zhang F, Yu X. Electrical percolation of nanoparticle-polymer composites. Comput Mater Sci 2018;150:102–6.
[46] Fang C, Zhang J, Chen X, Weng GJ. Calculating the electrical conductivity of graphene nanoplatelet polymer composites by a Monte Carlo method. Nanomaterials 2020;10(6):1129.
[47] Bao W, Meguid S, Zhu Z, Weng G. Tunneling resistance and its effect on the electrical conductivity of carbon nanotube nanocomposites. J Appl Phys 2012;111(9):093726.
[48] Li C, Thostenson ET, Chou T-W. Dominant role of tunneling resistance in the electrical conductivity of carbon nanotube–based composites. Appl Phys Lett 2007;91(22):223114.
[49] Haghgoo M, Ansari R, Hassanzadeh-Aghdam M. Prediction of electrical conductivity of carbon fiber-carbon nanotube-reinforced polymer hybrid composites. Compos B Eng 2019;167:728–35.
[50] Choi HJ, Ihm J, Louie SG, Cohen ML. Defects, quasibound states, and quantum conductance in metallic carbon nanotubes. Phys Rev Lett 2000;84(13):2917.
[51] Gbaguidi A, Namilae S, Kim D. Monte Carlo model for piezoresistivity of hybrid nanocomposites. J Eng Mater Technol 2018;140(1).
[52] Sahli S, Tabellout M. Study of the electrical conductivity in fiber composites. Int J Multiphys 2010;4(2).
[53] Kirkpatrick S. Percolation and conduction. Rev Mod Phys 1973;45(4):574.
[54] McLachlan DS, Chiteme C, Park C, Wise KE, Lowther, SE, Lillehei PT, et al. AC and DC percolative conductivity of single wall carbon nanotube polymer composites. J Polym Sci B Polym Phys 2005;43(22):3273–87.
[55] Sarkar AK, Saha S, Ganguly S, Banerjee D, Kargupta K. Hydrogen storage on graphene using Benkeser reaction. Int J Energy Res 2014;38(14):1889–95.
[56] Liu G, Shi Y, Wang L, Song Y, Gao S, Liu D, et al. Reduced graphene oxide/polypyrrole composite: an advanced electrode for high-performance symmetric/asymmetric supercapacitor. Carbon Lett 2020;30(4):389–97.
[57] Coleman JN, Cadek M, Blake R, Nicolosi V, Ryan KP, Belton C, et al. High performance nanotube-reinforced plastics: understanding the mechanism of strength increase. Adv Funct Mater 2004;14(8):791–8.
[58] Fukuda H, Kawata K. On Young's modulus of short fibre composites. Fibre Sci Technol 1974;7(3):207–22.
[59] Voll M, Kleinschmit P. Carbon, 6. Carbon black. In: Ullmann's encyclopedia of industrial chemistry; 2000.
[60] Noh YJ, Pak SY, Hwang SH, Hwang JY, Kim SY, Youn JR. Enhanced dispersion for electrical percolation behavior of multi-walled carbon nanotubes in polymer nanocomposites using simple powder mixing and in situ polymerization with surface treatment of the fillers. Compos Sci Technol 2013;89:29–37.
[61] Mohiuddin M, Hoa SV. Estimation of contact resistance and its effect on electrical conductivity of CNT/PEEK composites. Compos Sci Technol 2013;79:42–8.
[62] Lu X, Yvonnet J, Detrez F, Bai J. Multiscale modeling of nonlinear electric conductivity in graphene-reinforced nanocomposites taking into account tunnelling effect. J Comput Phys 2017;337:116–31.
[63] Feng C, Jiang L. Micromechanics modeling of the electrical conductivity of carbon nanotube (CNT)–polymer nanocomposites. Compos Appl Sci Manuf 2013;47:143–9.
[64] Zare Y. Development of Halpin-Tsai model for polymer nanocomposites assuming interphase properties and nanofiller size. Polym Test 2016;51:69–73.